Multiobjective Analysis to Identify
Compromise Wellfield Pumping Policies

XIV World Water Congress

Recife, Brazil

September, 2011

Emery A. Coppola Jr.[1], Ferenc Szidarovszky[2], Steven Spayd[3], Mary M. Poulton[4] Eric Roman[3]

[1]NOAH, L.L.C., 610 Lawrence Road, Lawrenceville, New Jersey, 08648-4208, U.S.A, Phone (609) 434-0400, email: emerynoah@comcast.net. [2]Department of Systems and Industrial Engineering, University of Arizona, Tucson, Arizona 85721-0020 U.S.A. [3]New Jersey Geological Survey, P.O. Box 427, Trenton, New Jersey, 08625-0427, U.S.A. [4]Department of Mining and Geological Engineering, University of Arizona, Tucson, Arizona, 85721-0012 U.S.A.

Abstract

As competition for water resources grows, multiobjective optimization may help identify appropriate management policies, particularly when disparate stakeholders are involved with conflicting objectives. In this study, decision analysis was conducted on a public water supply wellfield to balance water supply needs with well vulnerability to contamination from a nearby contaminant plume. With few alternatives, decision makers must balance these two conflicting objectives. Using a transient simulation model for the wellfield consisting of artificial neural networks, a formal multiobjective optimization model was developed, from which the Pareto frontier or trade-off curve between water supply and wellfield vulnerability was determined. Relative preference values and power factors were assigned to the three stakeholders, A compromise pumping policy that effectively balances the two conflicting objectives in accordance with the preferences of the three stakeholder groups was then identified using various distance-based methods. The above methodology can have many other applications to real-time adaptive water resources management.

Keywords: ground water management, artificial neural networks, multiobjective optimization

Introduction

Multiobjective decision analysis was applied to a real-world public supply wellfield, where the optimal tradeoff between water supply volume and vulnerability to ground water contamination was identified in accordance with the preferences and political powers of three stakeholder groups. Artificial neural network (ANN) derived state-transition equations served as the ground water flow simulator, which facilitated efficient and accurate computation of the Pareto frontier, depicting the trade-off curve between the two conflicting objectives. The ANNs, developed with simulation data from a numerical ground water flow model developed by the New Jersey Geological Survey (NJGS) for the study area, were embedded into an optimization program. The set of ANN-derived state-transition equations is an extremely condensed but highly accurate surrogate model for the 77,000 plus finite difference equations that constitute the numerical ground water model.

ANNs can help overcome erroneous solutions and/or computational inefficiencies that can occur when performing optimization with numerical models. Erroneous solutions may occur when the commonly used response coefficient methodology is applied to a non-linear (i.e. unconfined) ground water optimization problem. Riefler and Ahlfeld (1996) found that perturbation values for an unconfined problem that are either too large or too small can produce an erroneous solution. To avoid these perturbation problems, the generally less efficient embedding optimization approach can be used, where the ground water simulation model (i.e. numerical equations) is embedded into the optimization formulation as constraints. The ANN derived state-transition equations, used in lieu of a numerical model, can reduce the number of equations in the constraint set by orders of magnitude. Fewer mathematical operations are then required during optimization, not only increasing computational efficiency, but also minimizing round-off and precision errors that result from large numbers of mathematical operations (Szidarovszky and Yakowitz, 1978).

Also, given recent research, the concept of using ANN-derived state-transition equations as the simulation model has a potentially greater benefit for ground water optimization management. ANN models developed with real-world data have achieved high predictive accuracy for a number of complex hydrogeologic settings. Using real-world pumping, weather, and water level data, Coppola et al. (2003a,b; 2005a) developed ANN models that accurately predicted transient ground water levels at locations of interest (e.g. monitoring wells), and extended this to ground water quality (Coppola et al., 2005b). This work demonstrates that ANN models trained with real-world data can accurately predict dynamic ground water states at site-specific locations over discrete pumping management periods, which can exceed the accuracy of physical-based (e.g. numerical) models.

ANNs have the significant advantage, as demonstrated in this study, of not requiring difficult to estimate hydrogeologic parameters, like hydraulic conductivity and areal recharge, which often vary significantly over space and/or time. Instead, unlike traditional physical-based models, ANNs use more accessible and less uncertain input variables. In addition, because of their powerful non-linear modeling capability, ANNs are not limited by simplifying physical and/or mathematical assumptions (e.g. linear Darcian flow). A further advantage

is that the ANN-state transition equations can easily be initialized to the actual real-time conditions (e.g. water levels) measured in the field. By using more accurate state-transition equations in the constraint set and/or objective function in optimization problems, the computed optimal solution by extension, is more accurate.

In the area of multiobjective analysis, this study differs from related ground water literature (e.g. Willis and Liu, 1984; Yazicigil and Rasheeduddin, 1987; Shafike et al., 1992; El Magnouni and Treichel, 1994; Cieniawski et al., 1995; Freeze and Gorelick, 1999; McPhee and Yeh, 2004) in that the preferences of the primary stakeholders and their perceived political powers are explicitly accounted for in the decision-making process using various distance-based multiobjective methods. The study demonstrates the utility of this multiobjective optimization methodology to contentious and scientifically complex problems, and can be applied to similar water resources management problems.

There is a large body of literature that addresses single-objective ground water management optimization problems, with an extensive overview found in Gorelick (1983) and Ahlfeld and Mulligan (2000). Although most ground water optimization problems are solved with a single objective formulation, most real-world ground water management problems include multiple objectives. There are only a few published studies that consider formulating the ground water management problem within a formal multiobjective framework, where the Pareto frontier, which defines the trade-off curve between two or more conflicting objectives, is defined.

Typically, there are discrepancies between the preferences of the decision-makers and the stakeholders, and failure to adequately account for stakeholder attitudes could result in a solution that while technically feasible, is not socially appropriate and/or politically acceptable. Without clear regulatory or technical policies and in a contentious atmosphere as this study (Time magazine, 1999), the major challenge is identifying the "compromise" solution or optimal tradeoff between conflicting objectives, given the preferences and political influence of the stakeholders. Multiobjective analysis permits the decision-makers and stakeholders alike to quantitatively assess the tradeoffs between the conflicting objectives, and obtain a mutually acceptable compromise solution.

Toms River, a coastal New Jersey community, derives a large portion of its drinking water from the Parkway Wellfield (Figure 1), which withdraws water from an unconfined aquifer. One mile north of the Parkway Wellfield is the Reich Farm Superfund site, where improper disposal of hazardous waste resulted in ground water contamination. The contaminated plume migrated towards the wellfield, contaminating two of the supply wells, with the four other Parkway wells remaining vulnerable to contamination. Because of high water use, and the availability of only a few alternative water sources, the decision-makers must balance water supply with well vulnerability to contamination. The stakes are compounded by a six year, $10 million dollar epidemiologic study completed in 2002, which concluded that prenatal exposure to contaminated Parkway well water over the years 1982 to 1996 was a risk factor for leukemia in female children living in the community (New Jersey Department of Health and Senior Services, 2003).
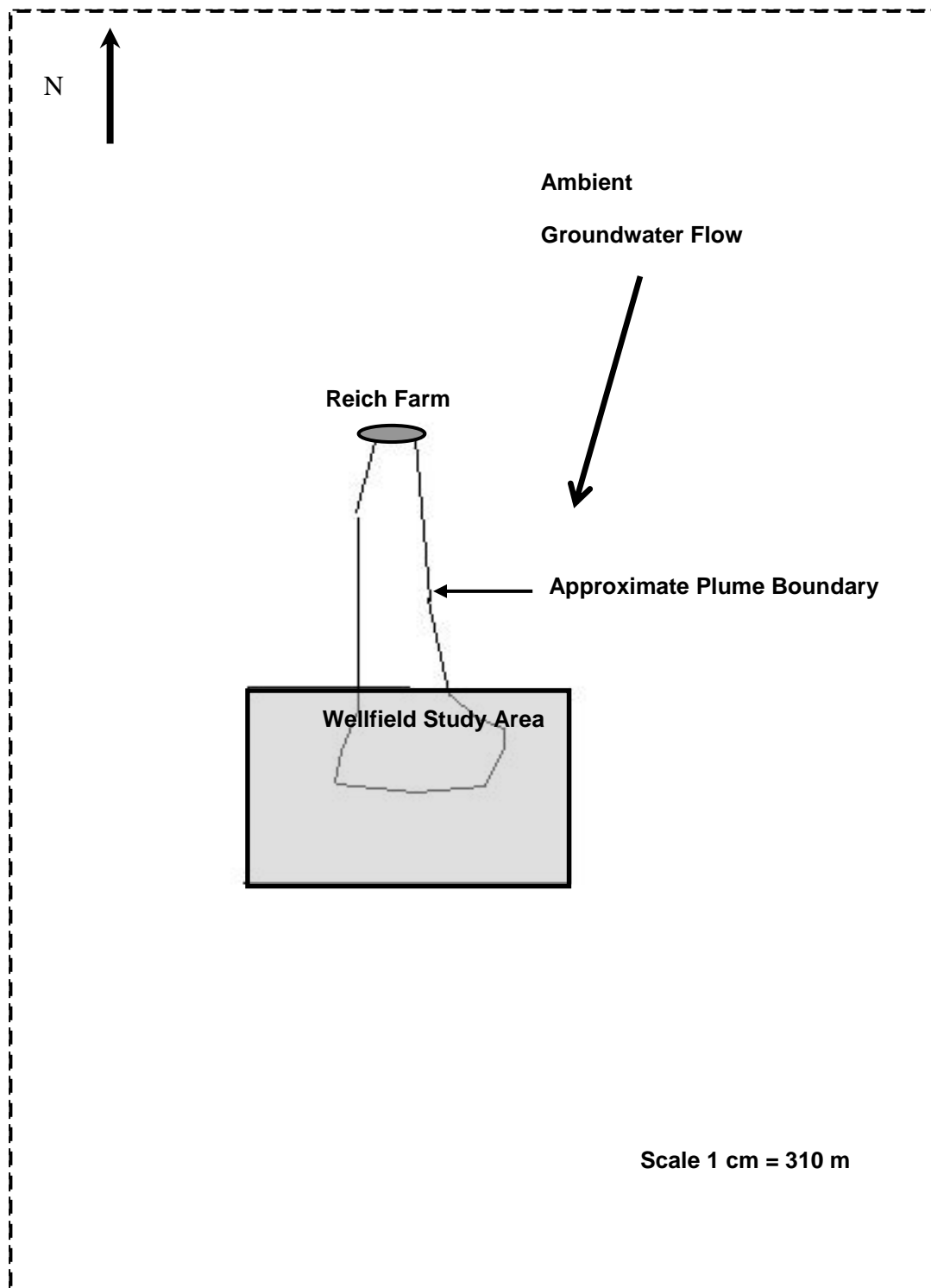
N

Ambient

Groundwater Flow

Reich Farm

Approximate Plume Boundary

Wellfield Study Area

Scale 1 cm = 310 m

Figure 1. Model boundary, plume, and wellfield area

The multiobjective analysis addressed the conflicting objectives of maximizing water supply via pumping extraction while minimizing well vulnerability to contamination over a 12-month planning horizon. In this study, vulnerability (Palmer et al., 1995; Satterfield et al., 2004), and wellhead protection concepts (United States Environmental Protection Agency, 1994) were combined to define vulnerability as the susceptibility of the four non-contaminated supply wells to the contamination plume, quantitatively measured as the sum of hydraulic head differences between corresponding cell locations, located on opposite sides of an approximated boundary that narrowly separates the plume from the vulnerable wells.

Using MODFLOW simulation data, ANN-derived state-transition equations were developed to accurately predict final heads for select cells at the end of monthly stress periods, as a function of initial heads, well pumping rates, and the real recharge rates over the duration of the stress period. The resulting state-transition equations were embedded into LINGO (LINDO, 1999), a commercial optimization program, to generate the Pareto frontier. Various multiobjective methods were then applied to identify the best compromise solutions.

Methods

The public supply wellfield is located within the Toms River basin, an area of temperate climate encompassing 319 square kilometers, located within the Atlantic Coastal Plain of New Jersey near the Atlantic Ocean. The basin overlies the unconfined Kirkwood-Cohansey aquifer system, a major regional source of water supply. The unconfined aquifer consists predominantly of coarse sand, intermixed with gravel and finer sediments, and is underlain by a thick low-permeability clay layer, which is considered a regionally confining layer. The strata dip gently seaward from west to east.

In the study area, the average distance from the ground surface to the water table is about 10 meters (m). Under non-pumping conditions, the saturated thickness of the unconfined aquifer is approximately 26 (m), and ground water flows in a general southwesterly direction. Analysis of an aquifer pumping test conducted at the wellfield and review of a limited number of tests in the area in conjunction with model calibration have produced estimated mean hydraulic conductivity and specific yield values of approximately 38 m/day and 0.25, respectively. Mean annual recharge into the aquifer, estimated from base-flow separation methods and numerical model calibrations, averages approximately 0.50 m per year.

The unconfined aquifer in the study area was modeled by the NJGS with MODFLOW (Harbaugh et al. 2000), the USGS finite-difference ground water flow code. The model was constructed to help perform a critical evaluation of earlier site models, as well as assess various pumping scenarios and develop Wellhead Protection areas for the Parkway Wellfield. The model domain measures approximately 4.4 by 5.6 kilometers, and consists of five layers, each discretized by 134 rows and 117 columns. The cell sizes are variable, with the interior cells around the Wellfield measuring roughly 10 by 10 m.

The proximal contaminant plume boundary, the six nearest of the eight pumping wells, and the fourteen ANN control cell locations used to quantify water level differences (i.e. vulnerability) along the plume boundary in layers 4 and 5 are depicted in Figure 2. Regulated organic compounds such as trichloroethylene (TCE) and tetrachloroethylene (PCE) are present in the ground water contaminant plume. This particular conflict resolution problem is further complicated as a number of identified chemicals present in the ground water plume are not regulated under the Safe Drinking Water Act, with the complete spectrum of hazardous chemicals illegally disposed at the site unknown. Although granular activated carbon treatment systems have been installed on the contaminated supply wells (Wells 26 and 28), as well as the two most vulnerable non-contaminated wells (Wells 22 and 29), this form of treatment may not remove all non-regulated contaminants potentially present in the plume.
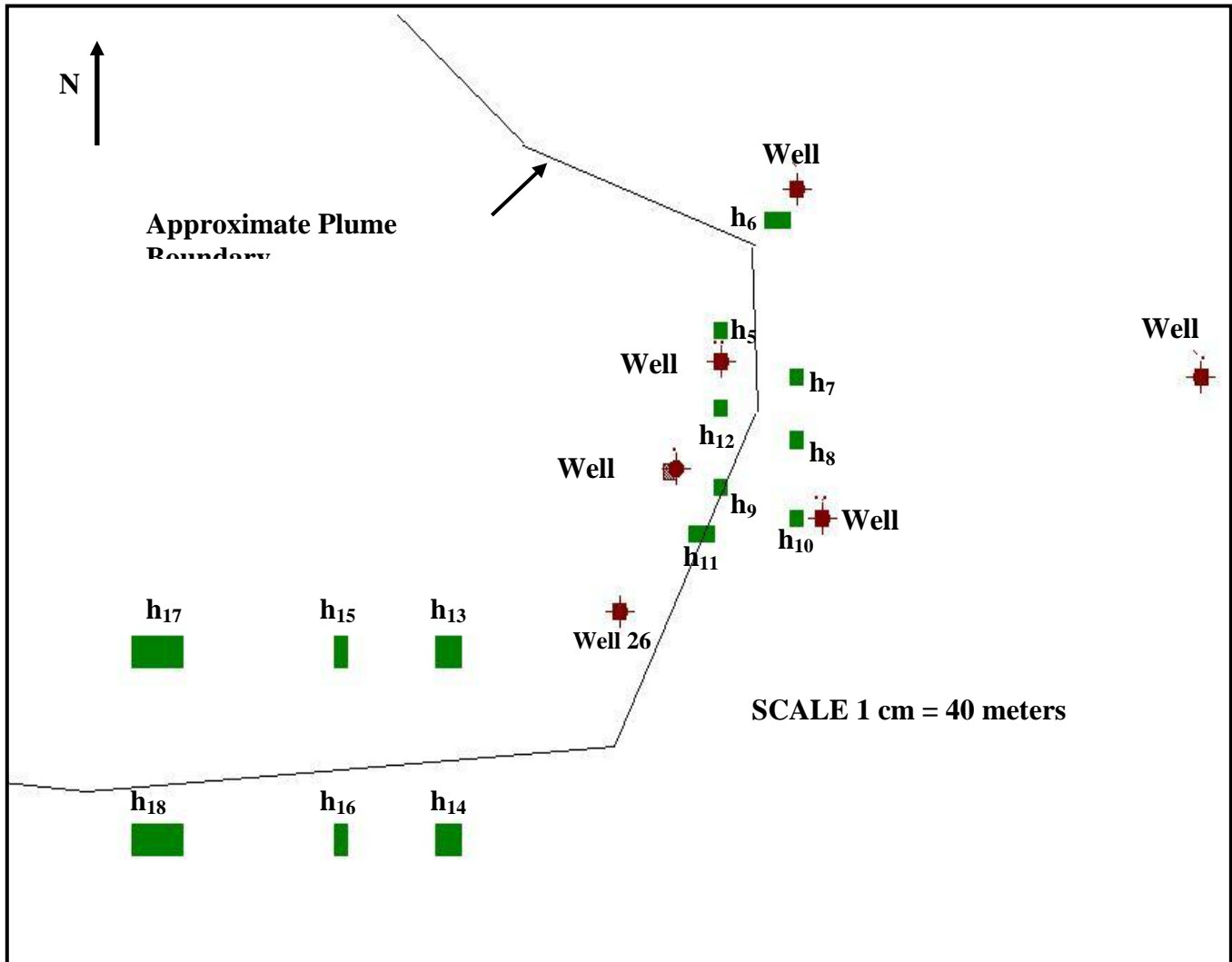
Figure 2.   Wellfield area depicting ANN control cell and well locations

In this ground water management problem, Wells 26, 28, and 26B (a subsequently installed recovery well), located within the contaminant plume, were constrained to pump at a cumulative rate of 4.54 m^3/min in accordance with treatment system constraints. Well 20, not part of Parkway and located peripheral to and relatively far from the plume, was constrained to pump at a constant rate of 1.51 m^3/min based upon numerical modeling and historical data. The conflicting objectives were to maximize the pumping rates of the four clean Parkway supply wells (Wells 22, 24, 29, and 44) while minimizing their vulnerability to contamination over an annual planning horizon, time-discretized into monthly stress periods.

Fourteen "control" cells, shown in Figure 2, were selected on both sides of the plume boundary. By pairing these control cell locations into "vulnerability pairs", the potential vulnerability of well contamination via plume migration could be evaluated for different pumping conditions. Because some pumping wells are screened in layer 4 and others in layer 5, vertical flow effects can be significant. Consequently, heads in both layers 4 and 5 were monitored at each of the control cells to quantify the potential vulnerability of well contamination as a function of head differences at twelve vulnerability pairs within the two layers, for a total of twenty-four vulnerability pairs. Please note that more than the fourteen cell locations were used in the ANN model; additional cells were used to help the ANN more accurately learn system responses to pumping and recharge stresses.

The vulnerability objective was quantified as the annual sum of the simulated water level differences between the "desired" downgradient and upgradient cells at the vulnerability pairs in both layers 4 and 5, which conform with the screened intervals of the pumping wells. For example, $V_{1,4,t}$ and $V_{1,5,t}$ represent the simulated water level (head) differences between the control cell locations at vulnerability pair 1 in layers 4 and 5, respectively, during month t. The subscript 1 in V simply denotes this as the first control pair, and subscripts 4 and 5 represent the layers. The head differences in both layers at this control pair during month t is explicitly expressed as:

$$V_{1,4,t} = h_{5,4,t} - h_{6,4,t}$$
$$V_{1,5,t} = h_{5,5,t} - h_{6,5,t}$$

where the first subscript in h indicates the assigned cell number, the second subscript denotes the layer, and the t subscript the month. A computed positive value for any vulnerability pair during any month t indicates that recovery well capture of the contaminant plume has not been achieved at this location, because the cell located outside of the plume boundary would have a lower head than its corresponding vulnerability cell within the plume area. For a given vulnerability pair, a higher number is indicative of a steeper hydraulic gradient (i.e. head difference), which would increase the rate and possibly the extent of the contaminant plume migration towards the downgradient supply well(s), increasing vulnerability to contamination. Conversely, a negative vulnerability value indicates hydraulic capture of the plume at the subject vulnerability pair in layer 4 during month t, the magnitude of which provides a relative measure of reduction in vulnerability. This sign convention applies to all control pairs in both layers.

Head difference rather than hydraulic gradient was selected as the vulnerability measure because it is a more intuitive concept for many stakeholders. Although hydraulic gradient would provide a more rigorous measure of potential vulnerability, given the spatial coverage of the vulnerability pairs, it was assumed that head differences provided an accurate relative measure of potential vulnerability, which was confirmed by MODFLOW simulations of the generated trade-off solutions.

As both objectives and all constraints are linear, the use of the weighting method with varying α weight values allows computation of the entire Pareto frontier (see for example, Szidarovszky et al. 1986), which is described in more detail later. Accordingly, the following multiobjective optimization model was repeatedly solved for α values between 0 and 1 for an annual planning horizon consisting of monthly stress periods:

Minimize [α * Vulnerability Measure Normed + (1 - α) * Supply Normed]   **(1)**

where

$$\text{Vulnerability Measure} = \sum_{j=1}^{12} \left(\sum_{t=1}^{12} V_{j,4,t} + \sum_{t=1}^{12} V_{j,5,t} \right) \qquad \textbf{(2)}$$

and

$$\text{Supply} = \sum_{t=1}^{12} (P22_t + P24_t + P29_t + P44_t). \qquad \textbf{(3)}$$

Notice that the vulnerability measure is the total sum of the (positive and negative) head differences and supply is the sum of the pumping rates over the entire 12-month period.

The following linear normalizing equations were used in the objective function:

Vulnerability Measure Normed =
(Vulnerability - MinVulnerability)/(MaxVulnerability - MinVulnerability)   **(4)**

and

Supply Normed = (MaxSupply - Supply)/(MaxSupply - MinSupply).   **(5)**

Model constraints included the minimum (i.e., 0 for all wells) and maximum feasible pumping rates for all decision variable wells, the imposed cumulative pumping rate constraint for the three recovery wells, and the fixed pumping rate for Well 20. The linear ANN-derived state-transition equations were included as additional management constraints for the linear optimization problem. For this multiobjective problem, there were 48 decision variables corresponding to the 12 monthly pumping rates, in m^3/min, for each of the four non-contaminated supply wells in the Parkway Wellfield. In addition, the optimal monthly pumping rates for each of the three recovery wells were computed by the linear optimization program.

Twelve multi-layered perceptron ANNs, each utilizing a back-propagation learning algorithm, were developed using MODFLOW simulation data. Coppola et al. (2005a, b) provide a detailed overview of artificial neural networks, including their general structural and functional forms, learning algorithms, and development issues.

Each ANN utilized forty-two inputs, consisting of initial ground water elevations at thirty-two MODFLOW model cell locations, monthly pumping rates of eight wells, monthly areal recharge rate, and a single bias unit. The outputs for each monthly ANN are the ground water elevations at each of the thirty-two cell locations. Twenty-eight of the locations pertain to the control cells, and the remaining four locations were selected to increase the accuracy of the ANN.

The ANN architecture selected utilized a single hidden layer, consisting of ten hidden nodes. Training was performed using 50,000 iterations, and the root mean squared error (RMSE) during training generally stabilized within 20,000 iterations. During training, the ANN processes training patterns consisting of input-output patterns through the network, systematically adjusting the connection weights, so that the measure of the overall goodness of the ANN model defined as the root mean squared error between the ANN-estimated output and the actual values converges to its minimum.

From forty-nine years of monthly ground water recharge values for the Toms River basin, five yearly sequences of recharge data representing both the extreme and mean recharge conditions were extracted.   These data were combined with 12,120 randomly generated monthly pumping patterns; each well withdrawing at a constant monthly rate, ranging from 0 to the maximum pump capacity of the well, with each rate independent of what the other wells pumped. The maximum pump capacity for all Parkway wells is 2.65 m^3/min, with the exception of Well 44, whose maximum capacity is 1.94 m^3/min. Using monthly stress periods, the ground water model was simulated for 12,120 consecutive stress periods, with heads in layers four and five saved. The combined data were split into two equal sets; the first was used to train the monthly ANNs, and the second for validation.

Despite nonlinear conditions associated with unconfined flow and partially penetrating pumping wells, accurate ANN results were obtained utilizing linear transfer functions. During validation of the 12 monthly ANN's, the difference between head values estimated by the ANN and actual MODFLOW were minimal, approaching 0. However, more importantly, in order to assess whether ANN prediction errors would accumulate during extended one-year simulations, the MODFLOW validation data was sequentially processed through the linked ANN-derived state-transition equations.

The monthly state-transition equations were sequentially linked so the evolution of head over the annual management period could be simulated. That is, for each year, the initial heads, pumping and recharge rates for January were processed through its state-transition equations to produce the final predicted monthly head values at the 32 locations. These final predicted head values for January were used to initialize the state-transition equations for February, and the corresponding pumping and recharge rates for this month were inputted to predict final monthly heads. This head initialization and data processing was repeated for the remaining ten months. The average head values predicted by the ANN functions for all months at the 32 head locations were compared with the MODFLOW generated values.

Ground water elevations at the ANN locations over the various stress periods ranged from approximately –3.0 to 12.0 m above mean sea level. The mean monthly head change at the 32 ANN locations was 0.70 m, with a maximum observed change of 9.3 m. Of the 384 mean head values (32 locations × 12 months), 247 estimated by the ANN matched exactly with the MODFLOW values, 136 differed by only 0.03 m, and the remaining one differed by only 0.06 m. The mean absolute error for all the head values was 0.03 m. From the 192,000 head comparisons made between the ANN estimated and MODFLOW simulated values, the maximum discrepancy was only 0.30 m. Overall then, the linked ANN achieved a high degree of accuracy in simulating the evolution of head at the nodal locations of interest over the one-year planning period.   Thus, the ANN's represents a highly accurate but condensed surrogate for the numerical ground water flow model at cells of interest.

Because the objective function and constraint set, including the ANN state-transitions, are all represented by linear equations or inequalities, they were embedded into LINGO (LINDO, 1999), and linear optimization was used to determine the Pareto solutions. Using initial head values obtained from MODFLOW and mean monthly recharge values, the objective function (1) was minimized for different α values.   In Eqn. (1), $\alpha = 1$ reduces it to the single objective of minimizing well vulnerability to contamination, which produces a total pumping supply of 0 over the annual planning period. In contrast, because of the form of Eqn. (5), setting $\alpha = 0$ in effect transforms the objective to maximizing water supply, producing both the maximum possible pumping extraction and the highest wellfield vulnerability to contamination. By systematically varying the value of α over the range [0, 1] and solving the corresponding optimization problem, the entire Pareto frontier was identified. In this two-objective case, the Pareto frontier is a 2-dimensional graphical representation of the trade-off between well supply and well vulnerability to contamination. The annual vulnerability values computed by the ANN were verified by MODFLOW simulation.   A comparison between the ANN-derived and MODFLOW-verified non-normalized Pareto frontiers is shown in Figure 3 and shows a very close match.
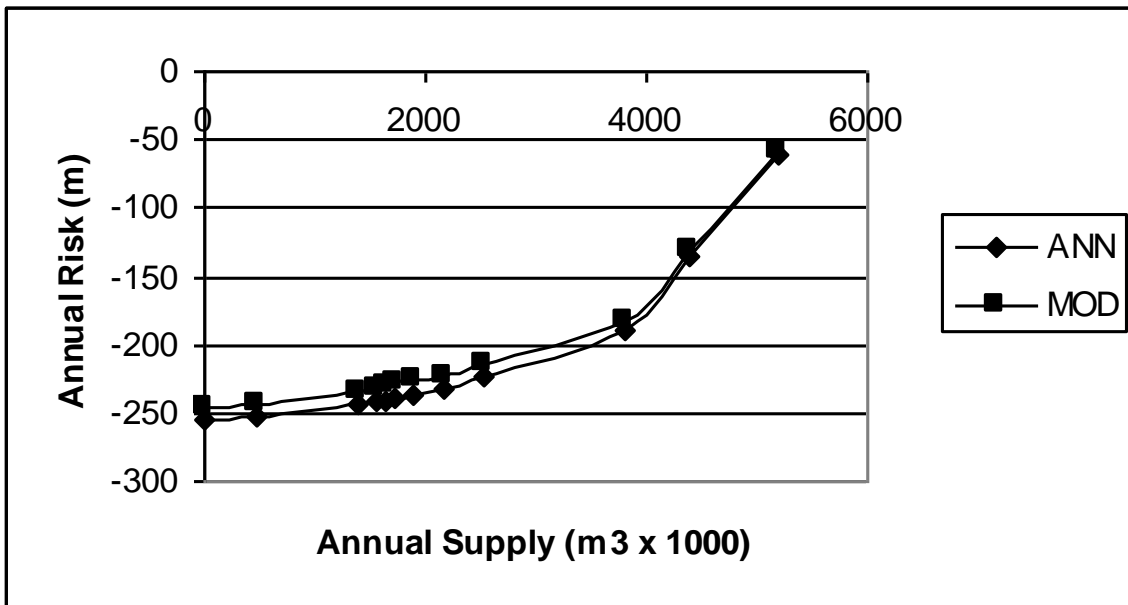

Figure 3. Non-normalized Pareto frontiers derived by ANN and verified with MODFLOW (MOD)

In the multiobjective optimization literature, distance-based methods are used most frequently for identifying possible optimal trade-off solutions. In this study, the following four traditional distance-based methods were used, with the ideal point representing the best of both objectives (non-attainable), and the nadir representing the worst of both objectives (also non-attainable). Thus, the ideal point is where water supply is maximum and

vulnerability is minimum, and the nadir point is the other extreme condition where supply is minimum (i.e. 0) and vulnerability to contamination is maximum.

Method 1: Minimize the distance from the ideal point based on the l_1 – metric.
Method 2: Minimize the distance from the ideal point based on the l_2 – metric.
Method 3: Minimize the distance from the ideal point based on the l_∞ – metric.
Method 4: Maximize the distance from the nadir point based on the l_2 – metric.

Generally, multiobjective techniques apply different metric measures for minimizing a specific distance from the ideal point and/or maximizing the distance from the nadir. A comprehensive summary of these methods is given in Szidarovszky et al. (1986).

Application of these methods requires weighing the relative importance of the objectives. For cases where decision-makers are unable to supply such weights, the computational results for a large set of systematically incremented pairs (w_1, w_2) can be presented to the decision-makers who can then assess their priorities based on the results. In a decision model like the one considered here, several interest groups (stakeholders) are involved.

Let K denote the number of interest groups and let $(w_1^{(k)}, w_2^{(k)})$ be the weights given by group k for k = 1, 2, …, K, for objectives one and two. These weights can be obtained by interviewing the members of the different groups independently. In an additional survey with the decision-makers or a government agency, the power factors $\alpha_1, \alpha_2, …, \alpha_K$ for each group are obtained such that $\alpha_1 + \alpha_2 + … + \alpha_K = 1$. Then the following final weight selections can be suggested:

$$w_1 = \sum_{k=1}^{K} \alpha_k w_1^{(k)} \quad \text{and} \quad w_2 = \sum_{k=1}^{K} \alpha_k w_2^{(k)}. \tag{6}$$

If for each group, $w_1^{(k)} + w_2^{(k)} = 1$, then the final weights w_1 and w_2 are also normalized: $w_1 + w_2 = \sum_{k=1}^{K} (\alpha_k w_1^{(k)} +$

$\alpha_k w_2^{(k)}) = \sum_{k=1}^{K} \alpha_k (w_1^{(k)} + w_2^{(k)}) = \sum_{k=1}^{K} \alpha_k = 1.$

Findings and Discussion

Figure 4 compares representative solutions derived from the MODFLOW and ANN-derived Pareto frontiers for two methods, namely minimizing the l_1 and l_2 distances.
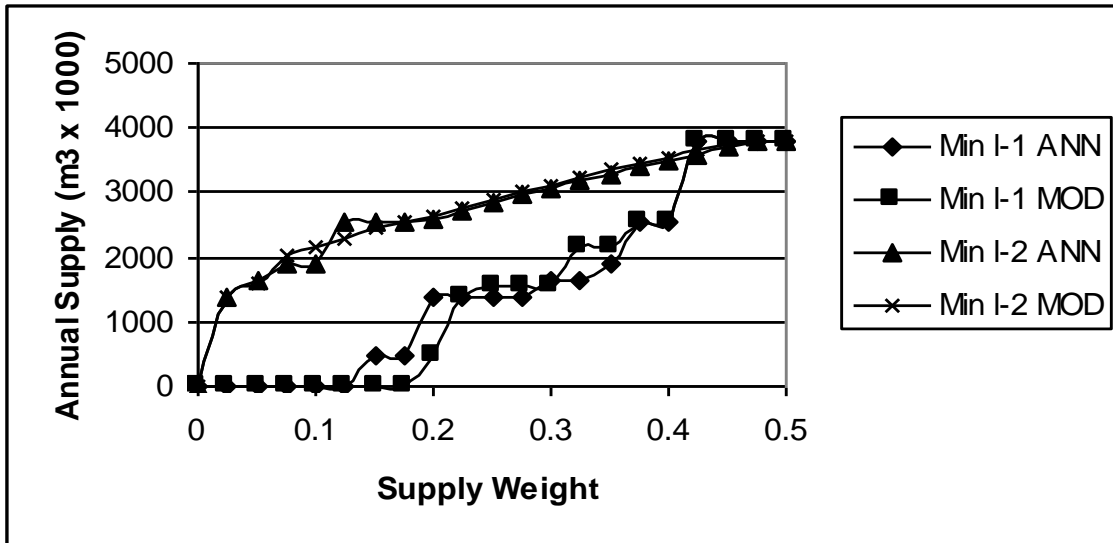

Figure 4. Multiobjective results from the MODFLOW (MOD) and ANN-derived Pareto frontiers obtained with the Min l_1 and Min l_2 distance-based methods

For all four methods, the solutions obtained from the two generated frontiers are in very close agreement. From these solutions, however, the optimal balance betweens supply and vulnerability must still be identified.

For this final analysis, preference weights and power factors were assigned to the three stakeholders. Ideally, the stakeholders would select the preference weights, and the power factors determined by a decision-making entity, such as the State or Federal environmental agency that is overseeing the water management problem. However, in this study, the weight selections and power factors were selected by the authors without input from either the stakeholders or the regulatory agencies, and as such, do not necessarily reflect the preferences of any of the involved entities. The weight preferences and power factors of the three stakeholders used in this analysis are listed in Table 1.

Table 1. Weight Preferences and Power Factors of Stakeholders.

Stakeholder	Supply w_1	Vulnerability w_2	Power Factor α_k
Community	0.2	0.8	0.6
Water utility	0.8	0.2	0.3
Chemical Manufacturer	0.4	0.6	0.1

In accordance with equation (6), the objective of well vulnerability to contamination is deemed the most important factor, and is given a final weight value of 0.6, compared with the 0.4 value computed for the objective of maximizing supply.   Under this solution, with the exception of the maximizing the l_∞ distance, the multiobjective methods produce similar results. Both Wells 24 and 44 pump at their maximum rates, and Well 29, most vulnerable to contamination, does not pump at all. Well 22 pumps anywhere from about 10 percent of its maximum rate to about 80 percent, with the mean value around 50 percent.

Coppola Jr.   11

Simulation of the resulting flow field under this pumping policy was performed with the MODFLOW model, with Wells 24 and 44 pumping at their maximum rates, and Well 22 pumping at about 50 percent of its maximum. The final contoured head field for layer 5 is depicted in Figure 5. Under this pumping policy, the contour lines generate flow paths that would converge to the recovery wells, protecting the clean wells from contamination. Similar flow paths result in layer 4, protecting wells from contamination.
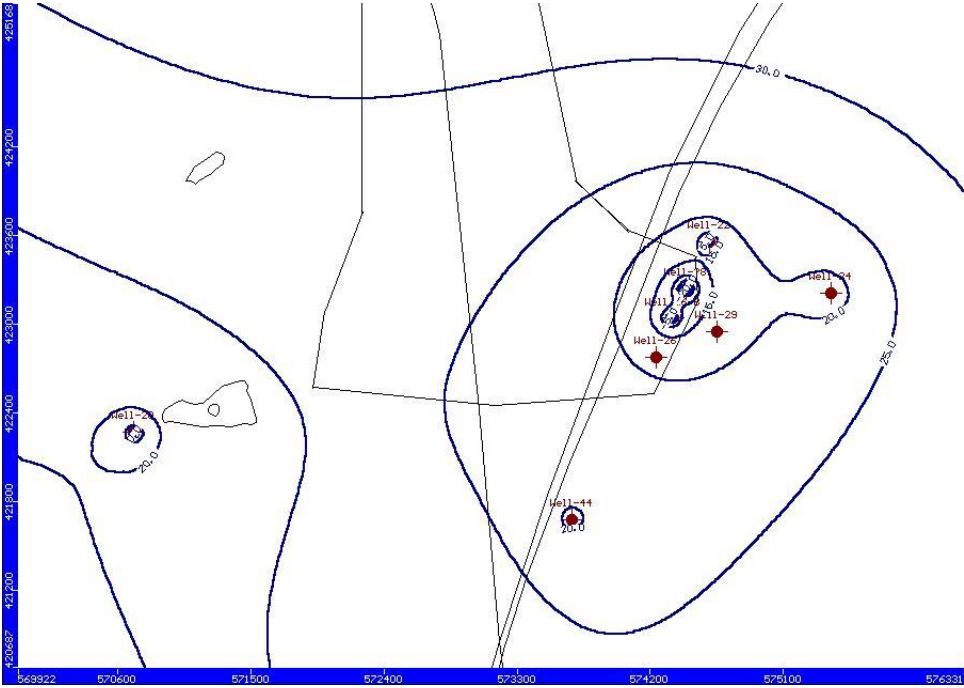

Figure 5. MODFLOW simulated water levels in layer 5 for optimal pumping policy, where the vulnerability objective weight = 0.6 and the supply objective weight = 0.4 (contour intervals in m above mean sea level)

As a comparison, the pumping policy for the case where vulnerability is equated equal to supply (i.e. weights of 0.5) was also simulated, with Well 22 now pumping at its maximum monthly rate. As Figure 6 shows, Well 22 appears slightly vulnerable to plume contamination.
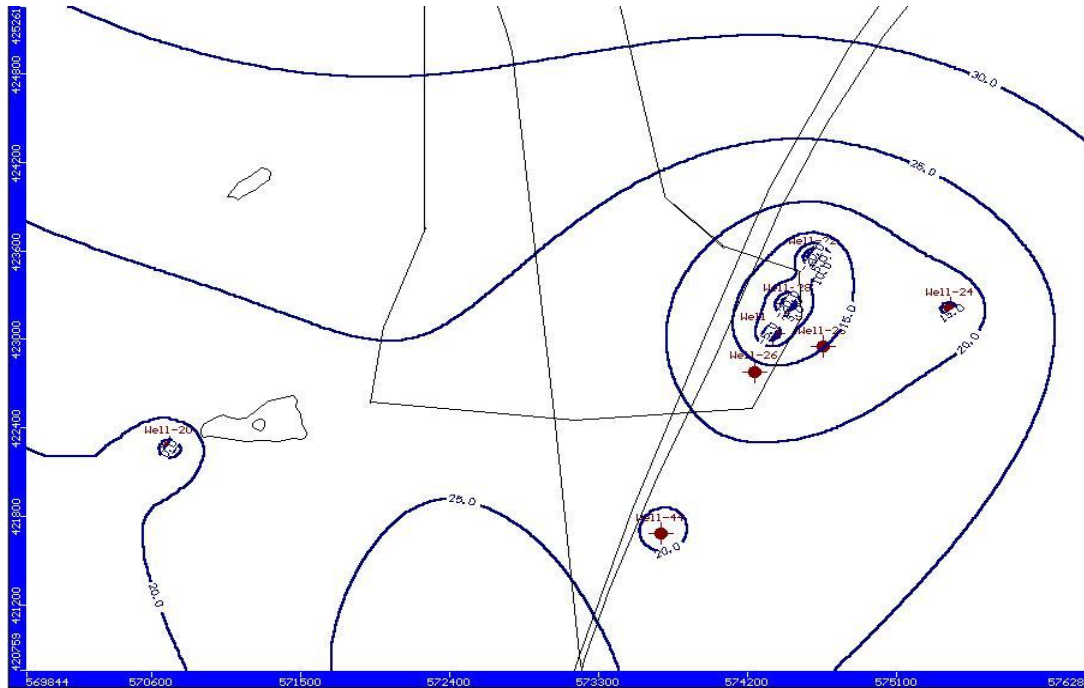
Figure 6. MODFLOW simulated water levels in layer 5, where the vulnerability objective weight = 0.5 and the supply objective weight = 0.5 (contour intervals in m above mean sea level)

However, when Well 22 pumping is reduced, hydraulic capture of the plume induced within this upgradient region is diminished, increasing vulnerability of Well 44.   This behavior illustrates the complex hydraulic interactions between supply wells located asymmetrically to an irregular plume boundary, where pumping rate changes of wells may increase vulnerability at some locations while decreasing it at others. The nominal increase of vulnerability at Well 44 under the optimal solution is more than compensated for by the reduction of the closer and more vulnerable Well 22, where the weight assigned to minimizing the vulnerability to contamination is 0.6.

This subtle but potentially critical shift from a vulnerability weight of 0.5 to 0.6 produced a compromise policy that effectively balances the assumed priorities of the various stakeholders. Under this policy, the water utility can operate the Wellfield at approximately 60 percent of its maximum, while satisfying customer concerns that the existing supply is being protected to the extent practicable. It is interesting to note how assigning a weight preference of 0.6 to vulnerability, which clearly places supply at a lower priority, still results in a supply reduction of only 40 percent from its maximum.   This may make the outcome more acceptable to the water utility, and leave stakeholders with the feeling that, given the complexity of the problem, and their conflicting priorities, an equitable compromise solution was achieved.

In summary, under the optimal operating policy derived with the assigned weight preferences and power factors, Wells 26B and 28 are used to control and recover the ground water contamination, and pump at 1.89 and 2.65 m^3/min, respectively. Of the non-contaminated Parkway wells, Well 22 pumps slightly under half its maximum monthly rate, at 1.27 m^3/min, Wells 24 and 44 pump at their maximum monthly rates of 2.65 and 1.94 m^3/min, respectively, and Well 29 remains shut-off.

Conclusions

The combination of ANN modeling with multiobjective optimization was applied to a complicated real-world ground water management problem in Toms River, New Jersey. This methodology serves as a formal framework for resolving conflict to the extent possible, and implementing a policy that best reflects the preferences and relative powers of the stakeholders. As water supplies become increasingly scarce during the 21st century, conflict between competing users will only become worse. Water disputes between various stakeholders, represented by such diverse interests as industrial, agricultural, residential, and environmental, to name just a few, each with different preferences and political power, may necessitate formal and rigorous conflict resolution analysis. Sandra Postel in her well known book *Last Oasis* (1997) argues that "a new water era has begun…marked by limits and constraints - political, economic, and ecological…and in many cases, achieving better water management will require decentralizing control over water, and moving from top-down decision making to greater peoples participation." Credible decision-making should often take into account trade-offs among various objectives in a rigorous and defensible manner, and as the competition for increasingly scarce ground water resources grows, policies may require true compromises.

Based upon previous research, the ANN models can be developed with real-world data and integrated directly with continuous data streams for real-time water resources prediction and optimization.

References

Ahlfeld, D. P., and Mulligan A. E. 2000. *Optimal Management of Flow in Groundwater Systems*, Academic Press, San Diego, CA.

Cieniawski, S. E., Eheart, J. W., and Ranjithan, S. 1995. "Using Genetic Algorithms to Solve a Multiobjective Ground Water Monitoring Problem." J. Water Resources Research, 31, no 2: 399-409.

Coppola, E., M. Poulton, E. Charles, J. Dustman, and F. Szidarovszky. 2003a. "Application of Artificial Neural Networks to Complex Groundwater Management Problems." J. Natural Resources Research, 12, no. 4: 303-320.

Coppola, E., F. Szidarovszky, M. Poulton, and E. Charles. 2003b. "Artificial Neural Network Approach for Predicting Transient Water Levels in a Multilayered Groundwater System Under Variable State, Pumping, and Climate Conditions." J. Hydrologic Engineering, 8, no. 6: 348-359.

Coppola, E., A. Rana, M. Poulton, F. Szidarovszky, and V. Uhl. 2005a. "A Neural Network Model for Predicting Water Table Elevations." J. Ground Water, 43, no 2: 231-241.

Coppola, E. C. McLane, M. Poulton, F. Szidarovszky, and R. Magelky. 2005b. "Predicting Conductance Due to Upconing Using Neural Networks." J. Ground Water, 43, no 6: 827-836.

El Magnouni, S., and Treichel, W. 1994. "A Multicriterion Approach to Ground Water Management." J. Water Resources Research, 30, no. 6: 1881-1895.

Freeze, R. A., and Gorelick, S. M. 1999. "Convergence of Stochastic Optimization and Decision Analysis in the Engineering Design of Aquifer Remediation." J. Ground Water, 37, no. 6: 934-954.

Gorelick, S. M. 1983. "A Review of Distributed Parameter Groundwater Management Modeling Methods." J. Water Resources Research, 19, no. 2: 305-319.

Harbaugh, A. W., Banta, E. R., Hill, M. C., and McDonald, M.G. 2000. "MODFLOW 2000, The U.S. Geological Survey Modular Ground Water Model-User Guide to Modularization Concepts and the Ground water Flow Process." U.S. Geological Survey Open-File Report 00-92.

LINDO Systems Inc. 1999. *LINGO 5.0 Users Manual*, Chicago, Illinois.

McPhee J. and Yeh, W.-G. (2004). "Multiobjective Optimization for Sustainable Groundwater Management in Semiarid Regions." J. Water Resources Planning and Management, 130, no. 6: 490-497.

New Jersey Department of Health and Senior Services in cooperation with Agency for Toxic Substances and Disease Registry, U.S. Department of Health and Human Services 2003. *Case-Control Study of Childhood Cancers in Dover Township (Ocean County), New Jersey. Volume I: Summary of the Final Technical Report.* www.state.nj.us/health/eoh/hhazweb/case-control_pdf/Volume_I/vol_i.pdf

Palmer, R.C., Holman, I.P., Robins, N.S., and Lewis, M.A. 1995. *Guide to Groundwater Vulnerability Mapping in England and Wales*, National River Authority, Bristol, United Kingdom.

Postel, S. 1997. *Last Oasis.* W. W. Norton & Company, Inc. New York, New York.

Riefler, R. G. and Ahlfeld, D. P. 1996. "The impact of Numerical Precision on the Solution of Confined and Unconfined Optimal Hydraulic Control Problems." J. Hazardous Waste and Hazardous Materials, 13, 167-176.

Satterfield,T.A., Mertz, C.K., and Slovic P. 2004. "Discrimination, Vulnerability, and Justice in the Face of Risk." J. Risk Analysis, 24, 115-129.

Shafike, N. G., Duckstein, L., and Maddock, T., III. 1992. "Multicriterion Analysis of Groundwater Contamination Management." AWRA Water Resources Bulletin, 28, no. 1: 33-43.

Szidarovszky, F., Gershon, E. M., Duckstein, L. 1986. *Techniques of Multiobjective Decision Making in Systems Management*, Elsevier, Amsterdam, Netherlands.

Szidarovszky, F. and Yakowitz, S. 1978. *Principles and Procedures of Numerical Analysis.* Plenum Press, New York, New York.

Time Magazine. 1999. Vol. 153 no. 2: 76-77.

United States Environmental Protection Agency 1994. *Groundwater and Wellhead Protection,* EPA/625/R-94/001.

Willis, R. and Liu, P. 1984. "Optimization Model for Ground-Water Planning." J. Water Resources Planning and Management, 110, no. 3: 333-347.

Yazicigil, H. and Rasheeduddin, M. 1987. "Optimization Model for Ground Water Management in Multi-Aquifer Systems." J. Water Resources Planning and Management, 113, no. 2: 257-273.